Cavity Catalysis: Modifying Linear Free-energy Relationship under Cooperative Vibrational Strong Coupling

*Jyoti Lather,[†] Thabassum Ahammad N. K.,[†] Jaibir Singh, and Jino George**

Department of Chemical Science, Indian Institute of Science Education and Research (IISER) Mohali, Punjab-140306, India.

ABSTRACT: Recent understanding of light-matter strong coupling brought a new niche in molecular-level control of chemical reactions. Vibrational strong coupling is unique in this category that overcomes the issue associated with coherent chemistry. Here, a vibrational transition is coupled to a standing wave of electromagnetic field, result in strong interaction, generating vibro-polaritonic states. This process reshuffles the entire energy-reaction coordinate. The chemical reaction rate can be boosted, stirred, or decelerated with this unconventional tool. Here, we used the idea of cooperative vibrational strong coupling of solute and solvent molecules to enhance the chemical reaction rate. This process is called cavity catalysis. Different derivatives of p-nitrophenyl benzoate (solute) and isopropyl acetate (solvent) are cooperatively coupled to an infrared Fabry-Perot cavity. The apparent reaction rates are increased by more than six times at the ON resonance condition, and the rate enhancement follows the lineshape of the vibrational envelope. Very interestingly, strong coupled system doesn't follow a linear free-energy relationship. The nonlinear rate enhancement can be due to the reshuffling of energy distribution between the substituents and the reaction center. Thermodynamic

parameters suggest an entropy-driven process for the coupled molecules. The free energy of activation decreased by 2-5 kJ/mol, suggesting a clear role of vibrational strong coupling in catalyzing the reaction. Here, the enthalpy of the system compensates for the entropy by preserving the isokinetic relationship. These findings will help further understanding of chemical reaction control in polariton chemistry.

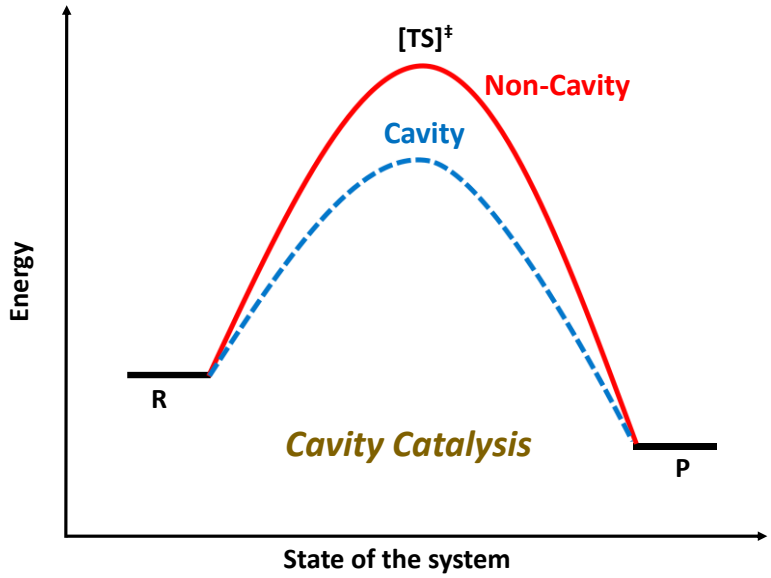

TOC

KEYWORDS: Light-matter strong coupling, polariton chemistry, Hammett relationship, isokinetic relationship, vibro-polaritonic states.

Introduction

The last decade witnessed progress in studying light-matter interaction in molecular systems.[1,2,3] Earlier, semiconductor researchers used this concept to understand the interesting properties of these hybrid, half-molecule-half-matter states. Recent experiments suggest that chemical and physical properties can be controlled precisely by coupling to vacuum electromagnetic field.[4] For example, room temperature Bose-Einstein condensation,[5] polariton lasing,[6] enhanced conductivity[7], etc., was the outcome of strong light-matter interaction.

Placing a molecular vibrational transition in an optical/plasmonic mode generates an exchange of photons when they come into resonance, creating two new eigenstates with equidistant energy from the fundamental transition called vibro-polaritonic states (*VP*+ and *VP*-; figure 1a).[8] The separation between the polaritonic states is called Rabi splitting ($\hbar\Omega_{VR}$), and the relation can be express as:

$$\hbar\Omega_{\mathrm{VR}} \propto 2d \cdot E \times \sqrt{n_{\mathrm{ph}} + 1}; \qquad E = \sqrt{\frac{\hbar\omega}{2\varepsilon_0 V}}$$

where, *d* is the transition dipole moment, and *E* is the electric field of the cavity mode. ε_0 is the vacuum permittivity, ω is the vibrational frequency, *V* is the mode volume of the cavity, and n_{ph} the number of photons involved in the coupling process. The interaction energy is still non-zero, even if $n_{ph} = 0$, called vacuum Rabi splitting.[9] This indicates that the zero-point energy of the molecule and the confined cavity mode directly exchange energy back and forth, even in the absence of an external photon. This idea of cavity quantum electrodynamic triggers a plethora of opportunities in chemical reaction dynamics. Due to half-molecule-half-matter behavior, the vibro-polaritonic state shows energy-momentum relation.[8] Another fascinating property of the system is the interaction energy can be tuned by varying the number of molecules coupled to the field. Here, $\hbar\Omega_{VR}$ is proportional to $\sqrt{N/V} \sim\sqrt{C}$, where *N* is the number and *C* the concentration of the coupled molecules.[10] This collective behavior is critical in observing changes in the chemical and physical properties of the coupled system.

Laser control of chemical reactions was a long-standing goal in coherent chemistry.[11] The availability of 3N-6 degrees of freedom makes an efficient distribution of energy within the system, decreases the quantum yield of a chemical conversion process.[12] Here, light-matter strong coupling offers a unique way to control the chemical reaction by constantly feeding energy through the vacuum field dressing of the upper and lower polaritonic states.[13,14] It also

provides the same effect without an external source, makes them promising for next-generation chemical reactors.[15] Ebbesen and co-workers proposed the first conceptual work in 2012 based on a photochemical reaction-switching of merocyanine to spiropyran-in a Fabry-Perot (FP) cavity.[16] The photochemical switching was slowed down due to the collective protection of the polaritonic states, thereby shifting the photostationary state. Here, the electronically excited state was coupled to the cavity mode. The above experiment seeded the idea of vibrational strong coupling (VSC) and helped to control chemical reactions at the molecular level. The first attempt in this direction was to couple C=O stretching band of a polymer, polyvinyl acetate, to an infrared FP cavity.[8] Later, many solids and liquids are shown to couple to the FP cavity.[17,18,19,20] The flow cell configuration of FP cavity is beneficial for homogeneous chemical reactions in the liquid state (figure 2).[21] The first experimental observation under VSC was a desilylation reaction.[22] Here, the reaction got decelerated at ON resonance coupling of C-Si band to an FP cavity mode. Selective coupling of C-Si band to the cavity mode decreased the reaction rate by more than four times at room temperature.[23] Another attempt was to try tilting the energy landscape through selective VSC of different functional groups in a molecule.[24]

This experimental observation generated a spur in the physical chemistry community as coherent chemical reaction control and improving the quantum yield was a dream for the researchers for decades. There were many theoretical approaches worldwide to understand the basic mechanism of cavity-mediated chemical reactions-called polariton chemistry.[25] In a first attempt, Feist and co-workers proved the collective nature of vibro-polaritons in chemical reactions.[26,27,28] A QE-DFT approach was also used to understand the potential energy surface and the reaction dynamics of small molecules like H_3^{+2} under VSC.[3] More theoretical papers appeared with suggestions on the dissipative nature and equilibrium consideration of VSC and their influence on reaction control.[29,30] Few spectroscopic experimental evidence suggests a

better energy transfer mechanism in the coupled system.[31,32] The vibro-polaritonic state can be used as a new decay channel in the reaction dynamics.[33,34] Other models such as the multi-level quantum Rabi (MLQR) model was introduced to understand the intermolecular interaction of the coupled molecules.[35] A very recent approach in this direction is the non-equilibrium behavior of VSC.[30] Even though there are significant attempts on the theoretical side, a general mechanism of polariton chemistry is not well understood.

There were very few attempts from the experimental side to understand the role of VSC on chemical reactions.[36] Hirai et al., shown that VSC can control a cycloaddition reaction.[37] Thermodynamic experiments suggest that the polarity of the C=O group got affected under VSC that decelerated the reaction rate. Charge transfer complexation of trimethylated-benzene–I_2 was studied, and the complexation equilibrium is shifting based on the symmetry of the vibrationally coupled state.[38] Another interesting work is to see the breaking of the Woodward-Hoffmann rule and the modification of stereoselectivity under VSC.[39] We have recently shown that cooperative VSC of solute to solvent molecules can drastically modify the chemical reaction rate.[40] A similar approach was also used to control enzyme hydrolysis by coupling to water molecules.[41] The main advantage of cooperative VSC is the bulk coupling of the solvent molecules in large numbers, thereby increasing the collective coupling strength and its effect on a chemical reaction.

Thermodynamic studies of all the chemical reactions under VSC show that the enthalpy and entropy of activation are drastically changing in the coupled system. Herein, we report cooperative VSC of a transesterification reaction decreases the free energy of activation by 2-5 kJ/mol, thereby catalyzing the reaction (figure 1b). Thus, the origin of cavity catalysis can be due to transition state (TS) stabilization triggered through better solvent reorganization. In the current work, we looked into the effect of substituents and the structure-reactivity relationship on the transesterification process of *p*-nitrophenyl benzoate molecules under VSC. The overall

idea is to study the linear free-energy relationship and other thermodynamic correlations to understand the mechanism of cavity catalysis.

Result and Discussion

The idea of cavity catalysis was materialized by the ergonomic design of an infrared microfluidic flow cell.[21] The cell is demountable, and a mylar spacer separates two substrates (windows) to complete the geometry of the flow cell-non-cavity. The spacer will define the pathlength, and it varies from 6-25 μm. The substrates mainly used for the experiments are BaF_2, CaF_2, ZnSe etc. Here, BaF_2 is selected for a specific reason to experiment in the UV-VIS to IR regime (BaF_2 is transparent from 0.2 μm to 10 μm in the wavelength spectrum). The inner side of the BaF_2 windows are sputtered with 10 nm Au mirrors to complete a Fabry-Perot design as shown in figure 2. All the experiments in cavity and non-cavity are conducted with a mylar spacer thickness of 12 μm. The FP cavity is designed to manually move the upper mirror by tightening and loosening the four screws on the top of the cell. The mirrors' flatness is ensured by observing Newton's rings formed in the center of the cavity structure (see the interference pattern formed in figure 2b). Please note that the elasticity of the spacer will allow moving the mirror precisely to achieve 1 cm^{-1} free spectra range (FSR) resolution. FSR can be calculated for the cavity using the formula $k(cm^{-1}) = \frac{10000}{2nL}$ where n is the refractive index (RI) of medium and L is the length between the mirrors (in μm). FSR value pre-calculated using the refractive index of the medium will help to attain ON resonance condition after injection of the reaction mixture. The cell design given in figure 2 is having a pathlength of one order of magnitude smaller than a conventional microfluidic setup. The smaller pathlength of the cavity forces us to work in a static configuration. The above design is unique and will help us study *in-situ* reaction kinetics while preserving the coupling condition.

Scheme 1: Scheme of ester solvolysis.

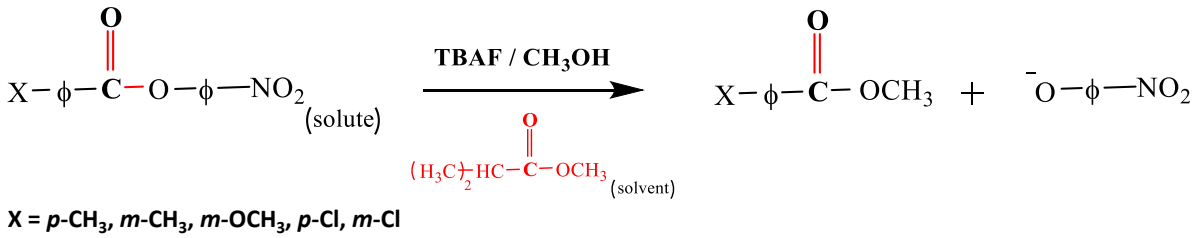

VSC of isopropyl acetate (IPAc) is achieved by coupling 7th mode of the cavity to the C=O stretching band (1739 cm^{-1}) of the solvent molecules. New vibro-polaritonic states (*VP*+ and *VP*-) are formed due to VSC, observed using an FTIR setup in the transmission mode configuration (figure 3a). Neat coupling of the solvent gives a Rabi splitting of 136 cm^{-1} with *VP*+ and *VP*- at 1814 cm^{-1} and 1678 cm^{-1}, respectively. VSC of liquid esters shows a similar coupling strength as reported in the literature.[40] There are five derivatives of *p*-nitrophenyl benzoate used for the experiment (Scheme 1). All the solute molecules selected have matching C=O stretching bands with respect to the solvent molecules. This allows the system to enter into cooperative VSC. Here, the solute concentration is 100 times lower than the bulk solvent, and hence the coupling strength is preserved during the course of the reaction. Angle-dependent measurements suggest a dispersive nature of polaritonic states with minimum energy at ON resonance condition. Vibro-polaritonic states and their spectroscopic studies are already known in the literature.[8] Our primary focus in the current work is to understand the influence of vibro-polaritonic states on the reaction rate.

Table 1: Apparent rate of the cavity and non-cavity experiments as plotted in Figure 5.

SL. No.	*Compound*	*C=O$_{str}$ (cm^{-1})*	*Non-cavity k_{app} (s^{-1})*	*Cavity k_{app} (s^{-1})*
1	PNPB	1744	1.05 x 10^{-3}	1.55 x 10^{-3}
2	*m*-CH$_3$	1742	7.73 x 10^{-4}	2.58 x 10^{-3}
3	*p*-CH$_3$	1741	5.54 x 10^{-4}	3.5 x 10^{-3}

4	*m*-OCH_3	1743	1.19×10^{-3}	1.86×10^{-3}
5	*m*-Cl	1748	1.63×10^{-3}	7.26×10^{-3}
6	*p*-Cl	1741	1.49×10^{-3}	$*7.5 \times 10^{-3}$

*Cavity experiments repeated two times at ON resonance condition, and the percentage error in k_{app} is ±16%

Stock solutions of *p*-nitrophenyl benzoate (0.1 M; PNPB) and all other derivatives (*p*-toluate (*p*-CH_3; *m*-toluate (*m*-CH_3); *m*-anisate (*m*-OCH_3); *p*-chlorobenzoate (*p*-Cl);); *m*-chlorobenzoate (*m*-Cl)) were prepared in IPAc, and tetrabutylammonium fluoride (0.1 M; TBAF) was prepared in methanol. All the derivatives are synthesized by following a reported procedure using substituted benzoyl chloride and *p*-nitrophenol.[42] The final products are characterized by IR and ^{1}H NMR spectroscopy. The solution containing solute molecules was prepared fresh and used for all the kinetic experiments. The final reaction mixture was prepared by mixing 190 µl of the solute and 10 µl of TBAF solution. The reaction mixture was immediately injected into an FP cavity (the FP cavity was kept at RT for about 30 minutes for stabilization before the injection) using a disposable syringe and studied the reaction rate at 400 nm in a UV-visible spectrophotometer (Cary-5000) for 600 seconds. The reaction follows a pseudo-first-order, base-catalyzed (B_{Ac2}) SN_2 mechanism.[43] The nucleophilic attack on the C=O carbon and formation of the negatively charged tetrahedral TS is the rate-determining step (RDS) of the reaction. The evolution of the spectra at 400 nm shows the formation of the product para-nitrophenoxide ion (PNP-). All the derivatives follow a similar reaction mechanism, whereas the substituents at *m*- and *p*- position control the reaction rate, either by inductive (±I) or/and by resonance (±R) effects.[42]

Kinetic traces obtained from the experiments conducted in the non-cavity condition for PNPB shows an apparent rate (k_{app}) of 1.05×10^{-3} sec^{-1} (k_H). The reaction rate changed approximately 1.5 times (1.55×10^{-3} sec^{-1}) in the cavity condition by coupling the C=O stretching band of the solute and solvent molecules. Similarly, we have conducted kinetic experiments for all the

derivatives in non-cavity and cavity conditions. k_{app} is increased from 1.5 times to 6 times for different substituents, as shown in Table 1. Very interestingly, moving the mirror position (FSR variation) from ON resonance to OFF resonance condition brings down the rate enhancement to non-cavity rate (Figure 4). The rate enhancement follows the vibrational envelope of the solute/solvent molecules, indicating a cooperative VSC mechanism. The same effect was reported previously by a similar class of molecules.[40] The rate enhancement lineshape changes slightly from *p*-Cl to *m*-CH_3 depending upon the position of the C=O stretching band.

Next, we have studied the rate enhancement ratio (k_X / k_H) for the cavity and non-cavity condition and compared it with the sigma (σ) (otherwise called substituent constant) of the benzoic acids. σ value is the difference in pK_a of unsubstituted to substituted benzoic acid.[44] σ value varies from negative to positive depending upon ±I and ±R effects of the substituents. Plotting log (k_X/ k_H) against σ value gives a straight line for the non-cavity system as it follows linear free-energy relationship, otherwise called Hammett relationship.[44] A linear regression fit will give the slope as reactivity constant (ρ). ρ value of PNPB based ester transesterification in IPAc is found to be +0.89. Please note that ρ value can vary depending upon the reaction condition and the solvent medium.[45]

Interestingly, experiments conducted in the cavity condition show breaking of linear free-energy relationship (here, all the experimental parameters are the same except the VSC effect). Substituents with σ_- show a negative ρ value, whereas σ_+ show a higher positive ρ value at the ON resonance condition. Here, the effect of the cavity can be complex; it not only modifies the electron density around the C=O group but also reshuffles the substituent effect at the reaction center by VSC. Please note that Hammett's empirical relation ignores the interaction of solvent molecules with different substituents (it only considers the dielectric constant of the solvent). Inductive and/or hyperconjugation effects are blocked in *p*-CH_3 and *m*-CH_3 under VSC,

resulting in an increased reaction rate. PNPB and *m*-OCH_3 show the minimal change in reaction rate, indicating that the energy distribution channel is not perturbed under VSC. At the same time, both *p*-Cl and *m*-Cl show a better stabilization of the TS by increasing its effective charge (ρ value is highly positive). Here, we assume that the σ value is not changing under VSC conditions; this approximation is essential to compare the structure-reactivity relationship in the cavity and non-cavity systems. The nonlinear behavior observed under VSC can be due to a change in the reaction mechanism or change in the RDS.[46] These aspects are further checked by looking into the thermodynamic behavior of the system.

Further, activation parameters are extracted for three of the substituents by carrying out temperature dependant studies. In the first case, a σ_- (*p*-CH_3) molecule is taken for the experiment. Eyring plot of the non-cavity sample shows the enthalpy and entropy of activation of 79.15 $kJmol^{-1}$ and -44.30 $JK^{-1}mol^{-1}$, respectively. The corresponding cavity at ON resonance condition shows the enthalpy and entropy of activation of 139.27 $kJmol^{-1}$ and +175.07 $JK^{-1}mol^{-1}$, respectively. The change in free-energy of activation ($\Delta\Delta G^{\ddagger}_{C\text{-}NC}$) from the cavity to non-cavity is found to be -5. 23 $kJmol^{-1}$. The fascinating observation here is that the entropy change is very high (219 $JK^{-1}mol^{-1}$), which is relatively large for any chemical reaction at a given condition. A detailed analysis of the enthalpy and entropy of activation is shown in Table 2. In the second case, σ_+ (*p*-Cl) molecule shows a very similar trend with a positive entropy of activation at ON resonance condition. *m*-OCH_3 molecules show the least variation as expected from the kinetic data; here also, the cavity coupling reshuffles the thermodynamic parameters as in the previous cases. The system enters into an entropy-driven process in the first two cases as $T\Delta\Delta S^{\ddagger}_{C\text{-}NC} > \Delta\Delta H^{\ddagger}_{C\text{-}NC}$ at RT (298 K). This observation is similar to solvent-triggered chemical reaction control in some of the reactions reported in the literature.[46,47]

Table 2: Thermodynamic parameters extracted from the linear regression fit of figure 6.

SL. No.	*Compound*	*σ*	$\Delta H^{\ddagger}_{NC}$ *(kJmol^{-1})*	$\Delta S^{\ddagger}_{NC}$ *(JK^{-1}mol^{-1})*	$\Delta H^{\ddagger}_{C}$ *(kJmol^{-1})*	$\Delta S^{\ddagger}_{C}$ *(JK^{-1}mol^{-1})*	$\Delta\Delta G^{\ddagger}_{C\text{-}NC}$ *(kJmol^{-1})*
1	*p*-CH_3	-0.17	79.15	-44.30	139.27	175.07	-5.23
2	*p*-Cl	0.23	53.53	-117.11	148.73	213.93	-3.17
3	*m*-OCH_3	0.12	83.53	-20.30	61.99	-90.03	-0.89

Now we try to compare the change in the thermodynamic parameters for the cavity and the non-cavity system. Plotting $\Delta\Delta H^{\ddagger}_{C\text{-}NC}$ against $\Delta\Delta S^{\ddagger}_{C\text{-}NC}$ gives a straight line indicating the reaction mechanism may not be affected as it follows isokinetic relationship.[48] The free energy of activation doesn't change much ($\Delta\Delta G^{\ddagger}_{C\text{-}NC}$ = 2-5 kJ/mol) as the entropy compensates for the enthalpy of activation. Please note that the Helmholtz free energy is not affected much under VSC as the zero-point energy shift is minimal. All these observations point to the fact that the vibrational control of the C=O stretching band by VSC can reshuffle the electron density locally in the reaction center and generate a non-equilibrium energy distribution, as evident from the breaking of the linear free-energy relationship. This non-equilibrium behavior may be originating from the control of electron density flow through inductive and resonance effects.

As evident from the kinetic and thermodynamic experiments, VSC plays a crucial role in controlling the chemical reaction dynamics in the system. Many factors can control reaction dynamics, which include: (i) intramolecular vibrational relaxation process within the solute molecule, (ii) intermolecular vibration distribution channel (self-interaction), and finally (iii) solute-solvent vibrational energy transfer. Cavity tuning experiments in figure 4 is a clear indication of the cooperative VSC effect. The rate enhancement follows the vibrational envelope suggesting a strong energy redistribution process with the cavity and the molecular

state. The first-order perturbation to molecular transition by cavity coupling (v_1 state of the figure 1a) may reshuffle its entire chemical reaction coordinate as suggested by many theoretical works.[3,49,50] The cavity resonance effect observed in three of the substituted derivatives (figure 4) pointing to the impact of the molecular level modification by cooperative VSC. At the same time, one can argue that a cavity can act as a thermal reservoir that can provide sufficient thermal energy to undergo multiple collision processes to overcome the barrier. This observation was already proved wrong by doing the experiments without strong coupling (in the absence of a strong oscillator), by only having the cavity mode as a reservoir.[40]

Now, let us look into the structure-reactivity relationship under VSC. The deviation from the linear free-energy relationship under VSC may have a different origin. Here, one can look into the electron density flow between the substituent and the reaction center through sigma and pi bonds. The electron-withdrawing and donating ability of the substituents plays a crucial role in the chemical reaction rate. Here, VSC of the C=O stretching band of the solute may favor/disfavor the electron density flow within the system, either through sigma or pi bonds. Previous experiments show that the resonance coupling of vibrational states to specific modes of the substituents can accelerate the energy transfer rate up to 50 times by controlling the IVR of *m*- and *p*-substituted derivatives.[51] VSC of the C=O band may increase the coupling state density of the substituents to the reaction center and provide a strong gateway for IVR within the coupled system. Another possibility is the play of a spectator bond or direct coupling of the substituents in the far IR region. The current experimental setup won't allow us to probe below 1000 cm^{-1}. *p*-CH_3 shows +R and +I effect; reaction rate gets amplified compared to *m*-CH_3 (+I effect), much faster than *m*-OCH_3 under VSC condition. On the other side, *p*-Cl and *m*-Cl has dominating -I effect also get amplified under VSC. Please note that the unsubstituted derivative shows the least variation among all the cases. This experimental observation is a strong argument on the role of VSC to control the electron density flow across the aromatic ring.

Thermodynamic experiments suggest that VSC brings an overall increase in entropy of activation. Simultaneously, a doubling of enthalpy of activation in *p*-CH_3, suggesting a change of mechanism. However, the linear correlation observed in $\Delta\Delta H^{\ddagger}_{C\text{-}NC}$ against $\Delta\Delta S^{\ddagger}_{C\text{-}NC}$ makes to believe the coupled system behaves similarly towards σ+ and σ– substituents. The isokinetic relationship observed here suggests a similar mechanism for cavity and non-cavity conditions. It is interesting to note that $T\Delta\Delta S^{\ddagger}_{C\text{-}NC} > \Delta\Delta H^{\ddagger}_{C\text{-}NC}$ (298K) indicates a pure entropy-driven process triggered through cooperative VSC. Along with that, the enthalpy-entropy compensation is a clear signature of cavity catalysis. Solute-solvent interaction is a complex phenomenon and understanding the kinetics and thermodynamics under VSC requires high-level theoretical intervention.

In conclusion, we observed the breaking of linear free-energy relationship in cavity catalysis by cooperative VSC of solute and solvent molecules. All the derivative of PNPB shows cavity catalysis, whereas the rate enhancement varies from one substituent to another. The nonlinear trend in the reaction rate can be due to IVR between the substituents and the reaction center. The origin of this can also be due to intra/intermolecular interactions.[52] Thermodynamics suggests a significant increase in entropy of activation to compensate for the enthalpy of activation. Here, cooperative VSC was used not only as a tool to understand the transesterification reaction of PNPB, but also to boost its chemical conversion. Selective coupling of vibrational bands to vacuum field and modification of chemical reaction with reasonable yield is now a reality. These experimental observations cement the concept of cavity catalysis and its application in chemistry.

AUTHOR INFORMATION

Corresponding Author

* jgeorge@iisermohali.ac.in

† these authors contributed equally.

ACKNOWLEDGMENT

We thank Prof. Srihari Keshavamurthy for his helpful discussions. DST-SERB, Core Research Grant (**EMR/2017/003455**), and MoE-Scheme for Transformational and Advanced Research in Sciences (**MoE-STARS/STARS-1/ 175**) are acknowledged for funding. J. L. thank IISER Mohali, T. A. NK thank DST inspire, and J. S. thank CSIR for the fellowships.

REFERENCES

1) Ebbesen, T. W. Hybrid Light–Matter States in a Molecular and Material Science Perspective. *Acc. Chem. Res.* **2016,** *49* , 2403-2412.
2) Hertzog, M.; Wang, M.; Mony, J.; Börjesson, K. Strong Light–matter Interactions: a New Direction Within Chemistry. *Chem. Soc. Rev.* **2019,** *48*, 937-961.
3) Flick, J.; Ruggenthaler, M.; Appel, H.; Rubio, A. Atoms and Molecules in Cavities, From Weak to Strong Coupling in Quantum-electrodynamics (QED) Chemistry. *Pro. Nat. Acad. Sci.* **2017,** *114*, 3026-3034.
4) Garcia-Vidal, F. J.; Ciuti, C.; Ebbesen, T. W., Manipulating Matter by Strong Coupling to Vacuum Fields. *Science* **2021,** *373*, eabd0336.
5) Plumhof, J. D.; Stöferle, T.; Mai, L.; Scherf, U.; Mahrt, R. F. Room-temperature Bose–Einstein Condensation of Cavity Exciton–polaritons in a Polymer. *Nat. Mater.* **2014,** *13*, 247-252.
6) Kena-Cohen, S.; Forrest, S. R. Room-temperature Polariton Lasing in an Organic Single-crystal Microcavity. *Nat. Photonics* **2010,** *4*, 371-375.

7) Orgiu, E.; George, J.; Hutchison, J. A.; Devaux, E.; Dayen, J. F.; Doudin, B.; Stellacci, F.; Genet, C.; Schachenmayer, J.; Genes, C.; Pupillo, G.; Samorì, P.; Ebbesen, T. W. Conductivity in Organic Semiconductors Hybridized with the Vacuum Field. *Nat. Mater.* **2015,** *14*, 1123-1129.

8) Shalabney, A.; George, J.; Hutchison, J.; Pupillo, G.; Genet, C.; Ebbesen, T. W. Coherent Coupling of Molecular Resonators with a Microcavity Mode. *Nature Commun.* **2015,** *6*, 5981.

9) Haroche, S.; Kleppner, D. Cavity Quantum Electrodynamics. *Phys. Today* **1989,** *42*, 24-30.

10) Brune, M.; Schmidt-Kaler, F.; Maali, A.; Dreyer, J.; Hagley, E.; Raimond, J. M.; Haroche, S. Quantum Rabi Oscillation: A Direct Test of Field Quantization in a Cavity. *Phys. Rev. Lett.* **1996,** *76*, 1800-1803.

11) Brumer, P.; Shapiro, M. Coherence Chemistry: Controlling Chemical Reactions with Lasers. *Acc. Chem. Res.* **1989,** *22*, 407-413.

12) Frei, H.; Pimentel, G. C. Selective Vibrational Excitation of the Ethylene–fluorine Reaction in a Nitrogen Matrix. I. *J. Chem. Phys.* ***2020*** **1983,** *78*, 3698-3712.

13) DelPo, C. A.; Kudisch, B.; Park, K. H.; Khan, S.-U.-Z.; Fassioli, F.; Fausti, D.; Rand, B. P.; Scholes, G. D. Polariton Transitions in Femtosecond Transient Absorption Studies of Ultrastrong Light–Molecule Coupling. *J. Phys. Chem. Lett.* **2020,** *11*, 2667-2674.

14) Scholes, G. D.; DelPo, C. A.; Kudisch, B. Entropy Reorders Polariton States. *J. Phys. Chem. Lett.* **2020,** *11*, 6389-6395.

15) Genet, C.; Faist, J.; Ebbesen, T. W. Inducing New Material Properties with Hybrid Light–matter States. *Phys. Today* **2021,** *74*, 42-48.

16) Hutchison, J. A.; Schwartz, T.; Genet, C.; Devaux, E.; Ebbesen, T. W. Modifying Chemical Landscapes by Coupling to Vacuum Fields. *Angew. Chem. Int. Ed.* **2012,** *51*, 1592-1596.

17) Long, J. P.; Simpkins, B. S. Coherent Coupling between a Molecular Vibration and Fabry–Perot Optical Cavity to Give Hybridized States in the Strong Coupling Limit. *ACS Photonics* **2015,** *2*, 130-136.

18) Simpkins, B. S.; Fears, K. P.; Dressick, W. J.; Spann, B. T.; Dunkelberger, A. D.; Owrutsky, J. C. Spanning Strong to Weak Normal Mode Coupling between Vibrational and Fabry–Pérot Cavity Modes through Tuning of Vibrational Absorption Strength. *ACS Photonics* **2015,** *2*, 1460-1467.

19) Hertzog, M.; Rudquist, P.; Hutchison, J. A.; George, J.; Ebbesen, T. W.; Börjesson, K. Voltage-Controlled Switching of Strong Light–Matter Interactions using Liquid Crystals. *Chem. Eur. J.* **2017,** *23*, 18166-18170.

20) Damari, R.; Weinberg, O.; Krotkov, D.; Demina, N.; Akulov, K.; Golombek, A.; Schwartz, T.; Fleischer, S. Strong Coupling of Collective Intermolecular Vibrations in Organic Materials at Terahertz Frequencies. *Nature Commun.* **2019,** *10*, 3248.

21) George, J.; Shalabney, A.; Hutchison, J. A.; Genet, C.; Ebbesen, T. W. Liquid-Phase Vibrational Strong Coupling. *J. Phys. Chem. Lett.* **2015,** *6*, 1027-1031.

22) Thomas, A.; George, J.; Shalabney, A.; Dryzhakov, M.; Varma, S. J.; Moran, J.; Chervy, T.; Zhong, X.; Devaux, E.; Genet, C.; Hutchison, J. A.; Ebbesen, T. W. Ground-State Chemical Reactivity under Vibrational Coupling to the Vacuum Electromagnetic Field. *Angew. Chem. Int. Ed.* **2016,** *55*, 11462-11466.

23) Thomas, A.; Jayachandran, A.; Lethuillier-Karl, L.; Vergauwe, R. M. A.; Nagarajan, K.; Devaux, E.; Genet, C.; Moran, J.; Ebbesen, T. W. Ground State Chemistry under Vibrational Strong Coupling: Dependence of Thermodynamic Parameters on the Rabi Splitting Energy. *Nanophotonics* **2020,** *9*, 249-255.

24) Thomas, A.; Lethuillier-Karl, L.; Nagarajan, K.; Vergauwe, R. M. A.; George, J.; Chervy, T.; Shalabney, A.; Devaux, E.; Genet, C.; Moran, J.; Ebbesen, T. W. Tilting a

Ground-state Reactivity Landscape by Vibrational Strong Coupling. *Science* **2019,** *363*, 615-619.

25) Yuen-Zhou, J.; Menon, V. M. Polariton Chemistry: Thinking Inside the (photon) Box. *Pro. Nat. Acad. Sci.* **2019**, 201900795.

26) Pino, J.-D.; Feist, J.; Garcia-Vidal, F. J. Quantum Theory of Collective Strong Coupling of Molecular Vibrations with a Microcavity Mode. *New J. Phys.* **2015,** *17*, 053040.

27) Galego, J.; Garcia-Vidal, F. J.; Feist, J. Suppressing Photochemical Reactions with Quantized Light Fields. *Nature Commun.* **2016,** *7*, 13841.

28) Galego, J.; Garcia-Vidal, F. J.; Feist, J. Many-Molecule Reaction Triggered by a Single Photon in Polaritonic Chemistry. *Phys. Rev. Lett.* **2017,** *119*, 136001.

29) Li, T.; Nitzan, A.; Subotnik, J. E. On the Origin of Ground-state Vacuum-field Catalysis: Equilibrium Consideration. *J. Chem. Phys.* **2020,** *152 23*, 234107.

30) Li, T. E.; Nitzan, A.; Subotnik, J. E. Collective Vibrational Strong Coupling Effects on Molecular Vibrational Relaxation and Energy Transfer: Numerical Insights via Cavity Molecular Dynamics Simulations. *Angew. Chem. Int. Ed.* **2021,** *60*, 15533-15540.

31) Xiang, B.; Ribeiro, R. F.; Du, M.; Chen, L.; Yang, Z.; Wang, J.; Yuen-Zhou, J.; Xiong, W. Intermolecular Vibrational Energy Transfer Enabled by Microcavity Strong light–matter Coupling. *Science* **2020,** *368*, 665.

32) Xiang, B.; Wang, J.; Yang, Z.; Xiong, W. Nonlinear Infrared Polaritonic Interaction Between Cavities Mediated by Molecular Vibrations at Ultrafast Time Scale. *Sci. Adv.* **2021,** *7*, eabf6397.

33) Campos-Gonzalez-Angulo, J. A.; Ribeiro, R. F.; Yuen-Zhou, J. Resonant Catalysis of Thermally Activated Chemical Reactions with Vibrational Polaritons. *Nature Commun.* **2019,** *10*, 4685.

34) Herrera, F.; Spano, F. C. Cavity-Controlled Chemistry in Molecular Ensembles. *Phys. Rev. Lett.* **2016,** *116*, 238301.

35) Hernández, F. J.; Herrera, F. Multi-Level Quantum Rabi Model for Anharmonic Vibrational Polaritons. *J. Chem. Phys.* **2019,** *151*, 144116.

36) Hirai, K.; Hutchison, J. A.; Uji-i, H. Recent Progress in Vibropolaritonic Chemistry. *ChemPlusChem* **2020,** *85*, 1981-1988.

37) Hirai, K.; Takeda, R.; Hutchison, J. A.; Uji-i, H. Modulation of Prins Cyclization by Vibrational Strong Coupling. *Angew. Chem. Int. Ed.* **2020,** *59*, 5332-5335.

38) Pang, Y.; Thomas, A.; Nagarajan, K.; Vergauwe, R. M. A.; Joseph, K.; Patrahau, B.; Wang, K.; Genet, C.; Ebbesen, T. W. On the Role of Symmetry in Vibrational Strong Coupling: The Case of Charge-Transfer Complexation. *Angew. Chem. Int. Ed.* **2020,** *59*, 10436-10440.

39) Sau, A.; Nagarajan, K.; Patrahau, B.; Lethuillier-Karl, L.; Vergauwe, R. M. A.; Thomas, A.; Moran, J.; Genet, C.; Ebbesen, T. W. Modifying Woodward–Hoffmann Stereoselectivity Under Vibrational Strong Coupling. *Angew. Chem. Int. Ed.* **2021,** *60*, 5712-5717.

40) Lather, J.; Bhatt, P.; Thomas, A.; Ebbesen, T. W.; George, J. Cavity Catalysis by Cooperative Vibrational Strong Coupling of Reactant and Solvent Molecules. *Angew. Chem. Int. Ed.* **2019,** *58*, 10635-10638.

41) Lather, J.; George, J. Improving Enzyme Catalytic Efficiency by Co-operative Vibrational Strong Coupling of Water. *J. Phys. Chem. Lett.* **2021,** *12*, 379-384.

42) Keenan, S. L.; Peterson, K. P.; Peterson, K.; Jacobson, K. Determination of Hammett Equation Rho Constant for the Hydrolysis of p-Nitrophenyl Benzoate Esters. *J. Chem. Edu.* **2008,** *85*, 558.

43) Mitton, C. G.; Schowen, R. L.; Gresser, M.; Shapley, J. Catalysis in ester cleavage. II. Isotope Exchange and Solvolysis in the Basic Methanolysis of Aryl Esters. Molecular Interpretation of Free Energies, Enthalpies, and Entropies of Activation. *J. Am. Chem. Soc.* **1969,** *91*, 2036-2044.

44) Hammett, L. P. The Effect of Structure upon the Reactions of Organic Compounds. Benzene Derivatives. *J. Am. Chem. Soc.* **1937,** *59*, 96-103.

45) Hansch, C.; Leo, A.; Taft, R. W. A Survey of Hammett Substituent Constants and Resonance and Field Parameters. *Chem. Rev.* **1991,** *91*, 165-195.

46) Cainelli, G.; Galletti, P.; Giacomini, D., Solvent Effects on Stereoselectivity: More than Just an Environment. *Chem. Soc. Rev.* **2009,** *38*, 990-1001.

47) Inoue, Y.; Ikeda, H.; Kaneda, M.; Sumimura, T.; Everitt, S. R. L.; Wada, T. Entropy-Controlled Asymmetric Photochemistry: Switching of Product Chirality by Solvent. *J. Am. Chem. Soc.* **2000,** *122*, 406-407.

48) Linert, W.; Jameson, R. F. The Isokinetic Relationship. *Chem. Soc. Rev.* **1989,** *18*, 477-505.

49) Ruggenthaler, M.; Tancogne-Dejean, N.; Flick, J.; Appel, H.; Rubio, A. From a Quantum-Electrodynamical Light–matter Description to Novel Spectroscopies. *Nature Rev. Chem.* **2018,** *2*, 0118.

50) Li, X.; Mandal, A.; Huo, P. Cavity Frequency-Dependent Theory for Vibrational Polariton Chemistry. *Nature Commun.* **2021,** *12*, 1315.

51) Timbers, P. J.; Parmenter, C. S.; Moss, D. B. Acceleration of Intramolecular Vibrational Redistribution by Methyl Internal Rotation. II. A Comparison of *m*-Fluorotoluene and *p*-Fluorotoluene. *J. Chem. Phys.* **1994,** *100*, 1028-1034.

52) Kadyan, A.; Shaji, A.; George, J. Boosting Self-interaction of Molecular Vibrations under Ultrastrong Coupling Condition. *J. Phys. Chem. Lett.* **2021**, *12*, 4313-4318.

Figures:

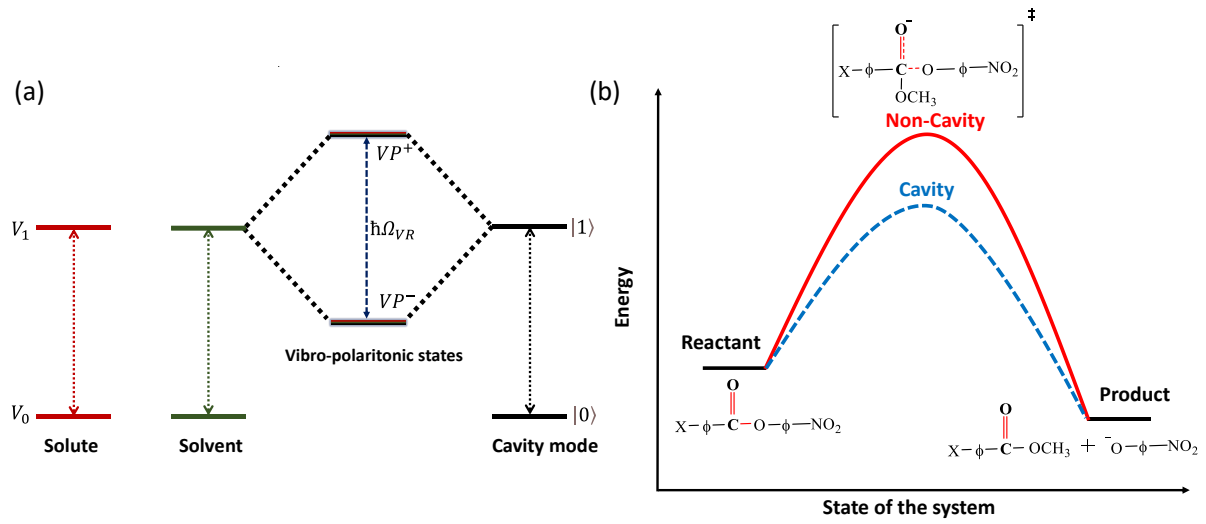

Figure 1: (a) Schematic illustration of cooperative VSC of solute and solvent molecules in a FP cavity. (b) A tentative energy diagram of change in free-energy of a chemical reaction in a cavity catalysis process.

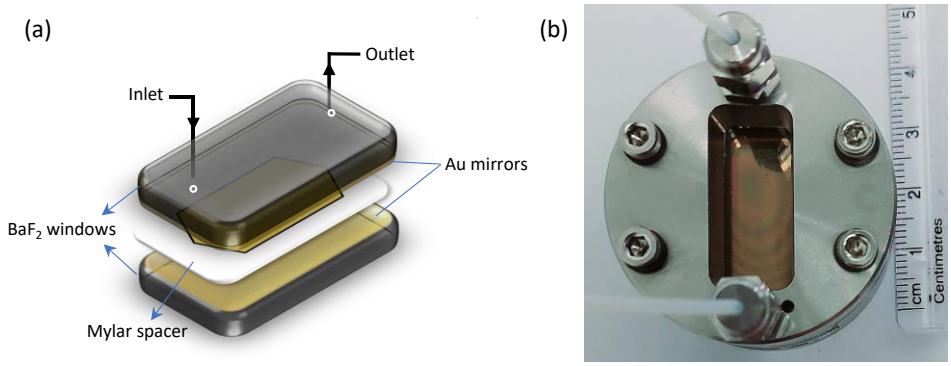

Figure 2: (a) Open sketch and (b) photograph of a FP cavity used for cavity catalysis experiment.

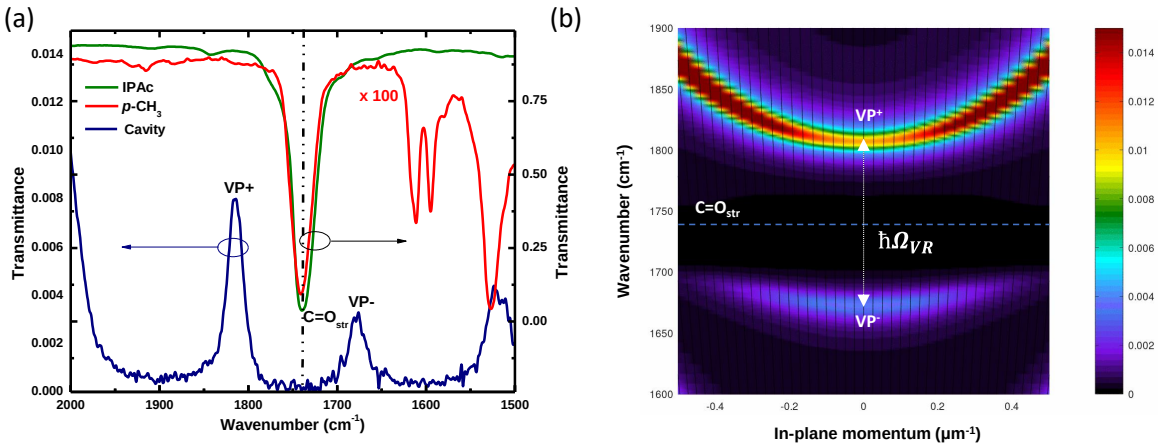

Figure 3: (a) FTIR spectra of neat isopropyl acetate (green trace), *p*-CH_3 in chloroform (red trace) and cavity at ON-resonance (blue trace) condition; (b) angle dependent dispersion measurement of $C{=}O_{str}$ band of solute and solvent molecules after coupling to 7th mode of an IR cavity.

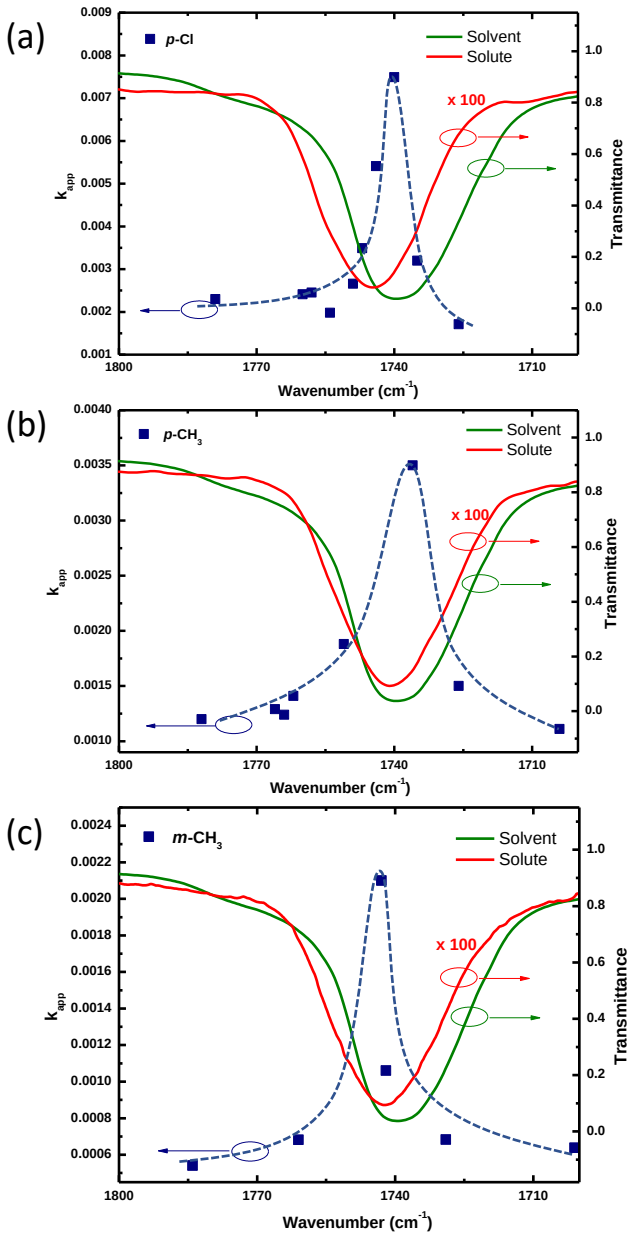

Figure 4: Kinetic action spectra for cavity catalysis measured at 298 K. Cavity mode position (7th) moved slowly from 1680 cm^{-1} to 1780 cm^{-1} in each experiment, and the corresponding k_{app} was plotted against the IR transmission spectra of C=O$_{str}$ band of solute (red trace) and solvent (IPAc; green trace) molecules. A sharp increase in the k_{app} was observed (blue square) at the ON resonance condition for (a) *p*-Cl, (b) *p*-CH$_3$, and (c) *m*-CH$_3$ in similar conditions [dotted lines are guide to the eyes].

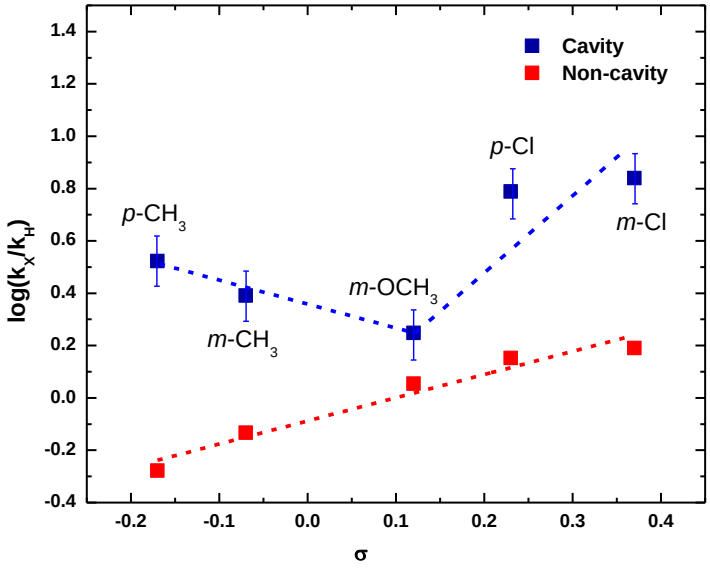

Figure 5: Hammett plot for a series of ester solvolysis (*p*-CH_3, *m*-CH_3, *m*-OCH_3, *p*-Cl, and *m*-Cl) in non-cavity (red squares) and ON-resonance cavity conditions (blue squares) [blue dotted lines are guide to the eyes; red dotted line is a linear regression fit].

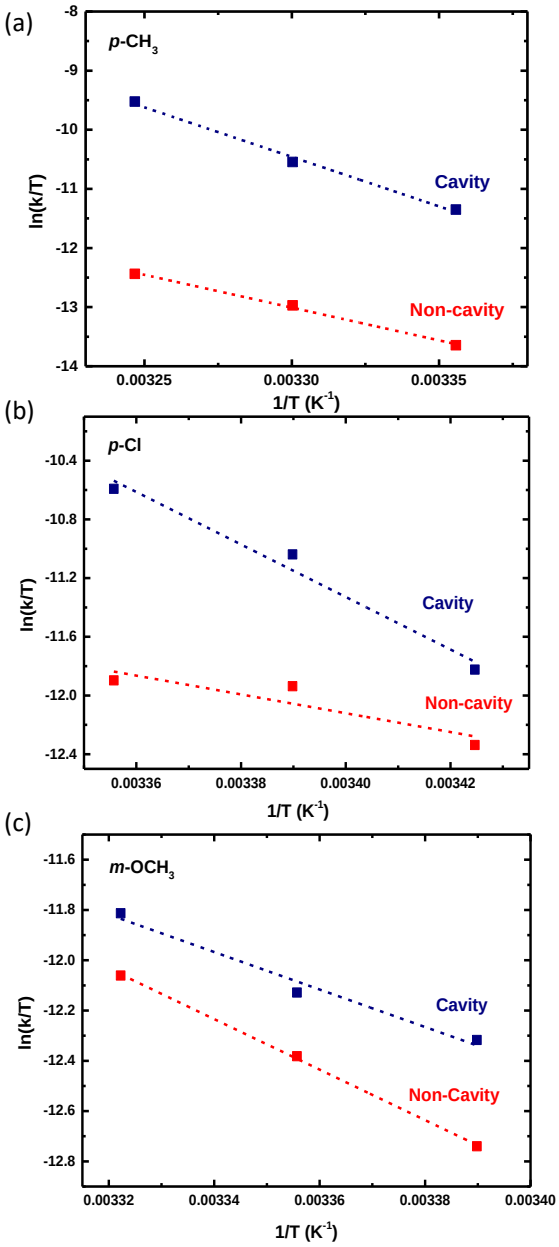

Figure 6: Eyring plot for k_{app} as a function of temperature in non-cavity (red squares) and ON-resonance cavity (blue squares) for (a) *p*-CH_3; (b) *p*-Cl; (c) *m*-OCH_3 under similar conditions.

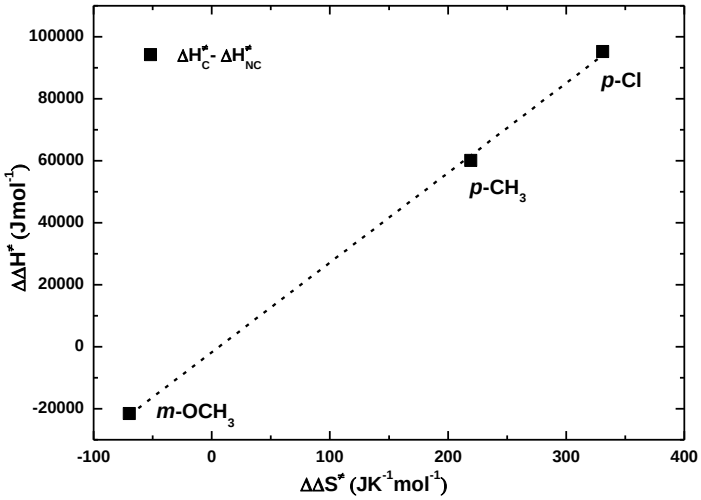

Figure 7: Enthalpy-entropy compensation plot for cavity *versus* non-cavity experiments listed in Table 2.